PAPER 73 (SESSION VI)

Brittle fracture strength of welded structures

K. IKEDA* and H. KEHARA†

*Chief, Materials Section, Ship Structure Division, Ship Research Institute, Tokyo, Japan.
†Professor of Naval Architecture, University of Tokyo, Japan.

Summary
A review is given of recent work in Japan on the relation of brittle fracture knowledge to engineering designs especially in the field of ship structures.

Introduction

It is necessary for the prevention of welded structures from brittle fracture to have the combinations of suitable materials, design and fabrication. In Japan, the WES (Japan Welding Engineering Society) Specification [1] has been applied to the weldable structural steel plates for those steel structures in which the brittle fracture should be taken into account. All major Japanese steel manufacturers marked the lowest allowable service temperature to their products under the approval by the society after completing more than 12 kinds of tests including various large and small scale brittle fracture tests and weldability tests.

The lowest service temperature was determined from the brittle fracture arresting characteristics for the specific arrested crack lengths which were taken to be average values in various specifications.

However, practically, the brittle fracture initiates at the weld defects or cracks existed in the welded joint. Therefore, the brittle fracture initiation characteristics of welded joint including bond and weld metal with notches, which are influenced by the kind of steel, the welding procedures, the welding heat input etc., is very significant.

The notches are classified as the through-thickness notch, the surface notch and the internal notch.

In addition, the welding residual stress at *T* type- or cross-joints, the angular distortion caused by mis-frabrication, the stress concentration due to structural discontinuity, the stress relieving heat treatment, the pre-strain, the strain rate etc. effects on the brittle fracture initiation characteristics.

Meanwhile, a brittle crack initiated at the welded joint propagates either into the base metal or along the welded joint under the effects of kind of steel, welding procedures and applied stress level.

Arrest of a propagating brittle crack at high speed can be realized by adopting the crack arrester. Recently, the effectiveness of crack arrester has been investigated systematically.

In this paper, the abstract of latest works in the field above mentioned is introduced briefly.

Brittle fracture initiation characteristics

Through-thickness notch

Base metal. Fracture initiation characteristics of steel plate with notch can be obtained by using the deep notch test specimens as shown in Fig. 1 [2]. In case of a mild steel (25 mm thick), the low stress brittle fracture occurs in the Region 1; the brittle fracture with general yielding, Region II; the ductile fracture, Region III, as shown in Fig. 2. In case of a 60 kg/mm² high strength steel (25 mm thick), Region II hardly exists as shown in Fig. 3.

In the region of low stress brittle fracture, the brittle fracture initiation is governed by the Griffith-Orowan energy equation, and the plastic surface energy for crack initiation, S_i, computed by equation (1) has a linear relationship with the absolute temperature as shown in Fig. 4 and expressed by equation (2)

$$\left.\begin{aligned} &\frac{\pi[f(\gamma)\sigma]^2 c}{2E} = S_i, \\ &f(\gamma) = \sqrt{\frac{2}{\pi\gamma}\left(\tan\frac{\pi\gamma}{2} + 0{\cdot}1\sin\pi\gamma\right)}, \\ &\gamma = c/b, \end{aligned}\right\} \quad (1)$$

$$S_i = S_{oi}\, e^{-2k_i/T_K}, \quad (2)$$

where, S_{oi}, k_i = material constant

Meanwhile, a linear relationship between the logarithm of yield stress and a reciprocal of absolute temperature exists as expressed by the following equation:

$$\sigma_y = \sigma_{oy}\, e^{k_y/T_K}, \quad (3)$$

where, σ_{oy}, k_y = material constant.

Now, let one take the safety factor, n, to the yield stress at the temperature concerned, the design stress is expressed by

$$\sigma = \frac{1}{n}\sigma_y. \quad (4)$$

The Griffith-Orowan energy equation for the initiation of unstable fracture for an infinite plate with a notch in length of 2c is expressed by the following equation:

$$\frac{\pi\sigma^2 c}{E} = 2S_i. \quad (5)$$

By combining equations (2) to (5), one obtains

$$\left.\begin{aligned} &e^{2(k_i+k_y)/T_K} = An^2 c \\ &A = \frac{2E}{\pi}\cdot\frac{S_{oi}^2}{\sigma_{oy}^2} \end{aligned}\right\} \quad (6)$$

The correlation between the half crack length, c, and the brittle fracture initiation temperature in absolute temperature, T_K, for an infinite plate is expressed by equation (6) and shown in Fig. 5 for mild steels, various high strength and low temperature structural steels presented in Table 1 at the stress level of $\sigma_y/2{\cdot}5$ [2].

Bond and weld metal [3]. In general, the bond in welded joint is more brittle than the base metal. Especially, it is believed that the embrittlement is pronounced in the 80 kg/mm² high strength steel. Of course, the degree of embrittlement depends on the heat input.

The brittle fracture initiation characteristics of bond and weld metal can be obtained by using the welded deep notch test specimen as shown in Fig. 6. In this specimen, the effect of residual stress can be neglected approximately, since the residual tensile stress in the direction perpendicular to the welded joint along the joint is relatively small and decreases by producing the notch.

For an example, the brittle fracture initiation characteristics of a 80 kg/mm² high strength steel was investigated. The fracture stresses or the modified gross stresses at fracture of bond, weld metal for the heat input of 13,000 (manual weld.), 35,000, 58,000 Joule/cm (Unionmelt weld.) vs. temperature curves are shown with the tensile strength and the yield stress in Fig. 7. The notch depth used is 120 mm. From the results, the brittle fracture initiation temperature of an infinite plate with various crack length can be obtained by the material constants and equation (6). For example, the correlation between the brittle fracture initiation temperature at the stress level of $\sigma_y/2{\cdot}5$ and the half crack length in an infinite plate for the bond, the weld metal and the base metal in case of the manual and the automatic weldings with heat inputs of 13,000 (manual), 35,000 and 58,000 (automatic) Joule/cm is shown in Fig. 8. It is noted that the embrittlement of bond by the automatic welding (submerged arc welding) is serious.

As an example of 60 kg/mm² high strength steels (HT60), the correlation between the brittle fracture initiation temperature and the half crack length for the bond and the weld metal with heat inputs of 15,000 (manual), 39,000 and 60,000 (automatic) Joule/cm is shown in Fig. 9. It is noted that the bond and the weld metal are unchanged irrespective of the manual and the automatic weldings. Therefore, the heat input control is not needed for the welding of HT60.

It is noted that the brittle fracture initiation temperature, T_i, increases with crack length. If the maximum crack length which might be overlooked at inspection after welding is assumed to be 80 mm, the half crack length of 40 mm is considered to be a fundamental crack length for evaluation of brittle fracture initiation temperature of steel quality. Consequently, the brittle fracture initiation temperature for 40 mm, $[T_i]_{c=40}$, is very significant. The difference of brittle fracture initiation temperature between bond and base metal, $[T_i]_{c=40}$ for various high strength steels, Steels A to M presented in Table 2, are shown in Figs. 10 and 11. The applied stress levels are 1/2·5 of the yield stress for base metal and bond at temperature concerned, respectively. It is noted that the heat input does not give any appreciable influence on the welding of HT60, and therefore, the heat input control is generally not necessary. Meanwhile, the embrittlement of bond becomes more serious when the heat input increases in automatic welding of HT70 and IIT80, although some HT80 is slightly affected by the heat input. In case of HT100, the heat input in manual welding does not effect on the embrittlement of bond.

The effect of stress relieving heat treatment on the steel quality and the effect of heat input on the brittle fracture initiation temperature were investigated, too.

Surface notch and internal notch [4, 5]

In general, the weld defects or the weld cracks existed in the welded joint are the surface notch or the internal notch. The brittle fracture initiation characteristics for through-thickness notch mentioned above is on the safety side from the viewpoint of service conditions.

In order to produce the internal notch with any notch depth-plate thickness ratio, the desired lack of penetration is used as shown in Fig. 12. In case of the surface notch, *Y*-type edge preparation is used on the Section *A-A*.

For a mild steel, the test specimens with notch of 80 mm long and depth-plate thickness ratio, t_1/t, of 0·1, 0·2, 0·3, 0·4, 0·6, 0·8, 1·0 were pulled in tension and fractured at low temperatures. The fracture stress-temperature curves for these specimens are shown in Fig. 13.

The correlations between the fracture stress and t_1/t at three temperatures are shown in Fig. 14. In the figure, the cases of internal and surface notches are expressed with the dotted and the solid curves, respectively. The fracture stress for $t_1/t = 1·0$ is that for deep notch test with through-thickness notch. The fracture stress for $t_1/t = 0$ is that for without notch or equal to the tensile strength in ductile fracture at the temperatures concerned. The fracture stress decreases abruptly as t_1/t increases from 0 to 0·2 or 0·3, and then does notch vary as t_1/t increases up to 0·6. When t_1/t is greater than 0·6, the fracture stress decreases steeply again. Consequently, the curves of brittle fracture initiation characteristics for surface or internal notches, which are found in the welded joint in welded structure, shifts to the lower temperature side in comparing with that for through-thickness notch ($t_1/t = 1·0$).

Welding residual stress [6]

The brittle fracture initiation characteristics of welded joint above-mentioned represents the steel quality in neglecting the welding residual stress. In cases of longitudinal and cross joints with a notch as shown in Fig. 15, the superposition of welding residual stress on the embrittled steel quality (bond or weld metal) results in higher brittle fracture initiation temperature.

Magnitude of tensile residual stress varies with kind of steel. The maximum tensile residual stresses for longitudinal and cross joints expressed as σ_1 and σ_2, respectively, as shown in Fig. 15 vary with kind of steel, and are presented in comparing with the yield stress, σ_y, in Table 3. It is noted that ratios of σ_1/σ_y and σ_2/σ_y decrease with strength of steel. Since the brittle fracture initiation characteristics of base metal, bond and weld metal are evaluated previously by the deep notch test in the form of plastic surface energy, the correlation between the brittle fracture initiation temperature and the half crack length can be calculated by combining the steel quality and the strain energy release rate for an enlarging crack superposed by any welding residual stress. An example of brittle fracture initiation temperature-half crack length curves for base metal and bond with and without residual stresses is shown in Fig. 16. The lowest service temperature can be safely determined from the highest temperature for an expected crack length on the brittle fracture initiation-half crack length curve with residual stress.

Structural discontinuity

There is a possibility of brittle fracture initiation at low stress levels when a notch exists in the region of structural discontinuity.

A theory of crack opening displacement using the model of dislocations, developed by Bilby, Cottrell, Swinden, has recently appeared before the footlight. The theory would be applicable even for the phenomenon of the initiation of brittle fracture initiation at considerably high stress levels such as the general yielding condition.

Recently, the theory of crack opening displacement was extended to the problems for arbitrarily distributed stress field and to apply successfully to analysis for the longitudinally welded *I*-type test as shown in Figs. 17 and 18 [9].

Angular distortion

The brittle fracture initiation characteristics above mentioned are related to the welded joint with no or slight angular distortion. Referring

to the brittle fracture casualty of *LPG* tank the effect of angular distortion caused by mis-fabrication on the brittle fracture initiation has been attracting attention.

Although the bond is considerably embrittled by the submerged arc welding with heat input of 45,000 Joule/cm for HT80 as suggested previously, the fracture stress-temperature curve shifts to the higher temperature side under the influence of angular distortion as shown in Fig. 19, and the phenomenon was analysed successfully from the viewpoint of critical strain [10, 11].

In addition, when the welding residual stress and the surface notch in various depths superpose on the angular distortion, as one of the severest service conditions, the fracture stress-temperature curve shifts to the higher temperature side further.

Crack path

In cases of mild steel, a brittle crack initiated at the bond or the weld metal curves to the base metal immediately as shown in Fig. 20 [12]. Therefore the crack arresting characteristics of bond or weld metal is out of problem.

The crack path for a 80 kg/mm² high strength steel welded manually or automatically is shown in Fig. 21 [3]. When the net stress on the notched section is higher than 43 kg/mm², a brittle crack propagates along the bond or in the weld metal.

Especially, a brittle crack always propagates straightly in the weld metal even when the net stress is as low as 22 kg/mm², in case of the heat input of 35,000 Joule/cm by the Unionmelt welding which results in the decreased brittle fracture strength. Main reason why the crack path curves to the base metal might be the stress distribution which is the superposition of applied stress on the welding residual stress. In case of the 80 kg/mm², the ratio of tensile residual stress to the yield stress is smaller than that for the mild steel. Therefore the effect of residual stress on the crack path for the high strength steel is less than that for the mild steel. In addition, since the brittle fracture strength of weld metal is less than that for the base metal, a brittle crack is inclined to propagate in the weld metal deposited by the submerged arc welding, the crack speed is greater than that by the manual welding or small heat input. When the crack speed is greater, the crack path might be less effected by the stress field.

In case of a 60 kg/mm² high strength steel, a brittle crack initiated at the bond or the weld metal deposited by the manual welding with the heat input of 15,000 Joule/cm curves to the base metal.

In case of the Unionmelt welding with the heat input of 35,000 Joule/cm, a brittle crack initiated at the bond curves to the base metal. On the contrary, a brittle crack initiated in the weld metal propagates

straightly in the weld metal as well as for the 80 kg/mm² high strength steel.

In case of a 70 kg/mm² high strength steel, a brittle crack initiated in the weld metal propagates straightly in the weld metal as well as for the 80 and the 60 kg/mm² high strength steel.

Of course, when the welded joint is stress relieved for any kinds of steel, a brittle crack always propagates straightly along the bond or in the weld metal, since the effect of welding residual stress cannot be found.

Brittle fracture arresting characteristics

The brittle fracture arresting characteristics of steel plate can be evaluated by using the double tension test or the ESSO test specimens of gradient and isothermal temperature types as shown in Fig. 22 [13, 14].

A linear relationship between the stress intensity factor for crack arrest, K_c (equation 7) and the absolute temperature, T_k, as shown in Fig. 23 [15] exists and is expressed by equation (8).

$$\left.\begin{aligned} K_c &= f(\gamma)\sigma\sqrt{(c)}, \\ f(\gamma) &= \sqrt{\frac{2}{\pi\gamma}\tan\frac{\pi\gamma}{2}}, \end{aligned}\right\} \tag{7}$$

$$K_c = K_{oc}\, e^{-k_c/T_K}, \tag{8}$$

where, K_{oc}, k_c = material constant.

The stress-arresting temperature curve for any arrested crack length, for example; 100 mm or 10 mm can be easily obtained.

Recently, evaluation of high quality steel as the crack arrester has been made by using the large size crack arrester test specimens in 30 mm thick., in which the distance of running brittle crack at high speed between the notch and the welded joint with crack arrester is 500, 750 and 1,000 mm, respectively, as shown in Figs. 24 and 25 [16]. It can be concluded in comparison with the results in standard size ESSO test with temperature gradient that the effective crack length for actual crack length of greater than 200 mm is not 100 mm as adopted in the WES specification, but should be greater than 100 mm as shown in Fig. 26. The greater specimen of 2,400 mm square and 20 mm thick in similar form to the specimen mentioned previously is being presently tested at the University of Tokyo, and the results are shortly expected.

The brittle crack is arrested when the stress intensity factor K is equal to K_c which were evaluated by the double tension test or the ESSO test with temperature gradient as shown in Fig. 27 [16]. In cases of the stiffener type and ditch type arresters, the theoretical and the experimental analyses have been developed [18, 19].

References

1. WES-Specification, Qualification of Steel Quality for Low Temperature Steel, Japan Weld. Eng. Soc., 1964.
2. IKEDA, K., AKITA, Y. & KIHARA, H. 'The deep notch test and brittle fracture initiation', *Welding Journal*, vol. 46, no. 3, pp. 133s-144s, 1967 I.I.W. Doc. no. W-404-67, 1967.
3. IKEDA, K. & KIHARA, H. 'Brittle fracture strength of welded joint'. To be presented at 1969 Annual Meeting of American Welding Society.
4. KIHARA, H., IKEDA, K. & SUSEI, S., MAENAKA, H. & MINAKATA, S. 'Effect of notch size on brittle fracture initiation' (First Report) – Experimental research on welded butt joint of mild steel, *Jnl. Soc. Nav. Arch. Japan*, vol. 122, pp. 174-190, 1967.
5. KIHARA, H., IKEDA, K., SUSEI, S., MAENAKA, H. & MINAKATA, S. Ditto. (Second Report) – On type of notch and fracture appearance, *Jnl. Soc. Nav. Arch. Japan*, vol. 123, pp. 253-262, 1968.
6. IKEDA, K., KANAZAWA, T. & KIHARA, H. 'Effect of welding residual stress on brittle fracture initiation', I.I.W. Doc. No. X-48-68, 1968.
7. KIHARA, H., IKEDA, K. & NARITA, K. 'Effect of stress concentration due to structural discontinuities on initiation of brittle fracture in low stress level', I.I.W. Doc. No. X-292-62, 1962..
8. AKITA, Y. 'Consideration with regards to brittle fracture at major discontinuity', IRC-III-26, 1963, (not published).
9. YADA, T. & SAKAI, K. 'A study on brittle fracture initiation from structural discontinuities in arbitrarily distributed stress field', *Jnl. Soc. Nav. Arch. Japan*, vol. 123, pp. 263-273, 1968.
10. AKITA, Y. & YADA, T. 'On brittle fracture initiation characteristic to welded structures' (Report No. 1) – Transversely welded wide plate test, *Jnl. Soc. Nav. Arch. Japan*, vol. 117, pp. 237-243, 1965.
11. AKITA, Y., MAEDA, T. & YADA, T. Ditto. (2nd Report), *Jnl. Soc. Nav. Arch. Japan*, vol. 118, pp. 171-191, 1965.
12. KIHARA, H., YOSHIDA, T. & OHBA, H. 'Initiation and propagation of brittle fracture in welded steel plate', I.I.W. Doc. No. X-217-59, 1959.
13. YOSHIKI, M., KANAZAWA, T. & MACHIDA, S. 'A Consideration on brittle fracture test of steel plates – with special reference to flat-temperature and gradient-temperature type double tension test', *Jnl. Soc. Naval Arch. Japan*, vol. 113, pp. 125-135, 1963.
14. AKITA, Y. & IKEDA, K. 'On brittle crack propagation and arrest – theoretical and experimental analyses of ESSO test with temperature gradient', I.I.W. Doc. No. IX-364-63, 1963.
15. KOSHIGA, F., IMAZAWA, O. & TAKEHANA, S. 'Arrest – transition of brittle crack in steel plate', *Jnl. Soc. Nav. Arch. Japan*, vol. 114, pp. 200-209, 1963.
16. KIHARA, H., KANAZAWA, T., IKEDA, K., MAENAKA, H. & KINOSHITA, M. *et al.* 'Effectiveness of crack arrester (First Report), *Jnl. Soc. Nav. Arch. Japan*, vol. 122, pp. 191-200, 1968.
17. KIHARA, H., KANAZAWA, T., IKEDA, K., MAENAKA, H. & KINOSHITA, M. *et al.*, Ditto. (Second Report), *Jnl. Soc. Nav. Arch. Japan*, vol. 124, 1968.
18. YOSHIKI, M., KANAZAWA, T. & MACHIDA, S. 'Some basic considerations on crack arresters for welded steel structures (The Third Report) – Experimental checks', *Jnl. Soc. Nav. Arch. Japan*, vol. 118, pp. 192-203, 1965.
19. KANAZAWA, T., MACHIDA, S. & OHYAGI, M. Ditto. (The Fifth Report) – with special reference to 'Ditch-type' and 'Stiffener-type' arresters, *Jnl. Soc. Nav. Arch. Japan*, vol. 122, pp. 200-214, 1967.

Table 1.
Chemical compositions and mechanical properties for steels tested

Steel	Kind of steel	Plate thick. mm	Chemical compositions													Mechanical properties		
			C	Si	Mn	P	S	Cu	Ni	Cr	Mo	V	B	Al	N_2	Y.P. (kg/mm²)	T.S. (kg/mm²)	Elong. (%)
A	Normalized killed	20	0·20	0·23	0·71	0·015	0·027									25·1	41·1	32·6
B	HW 36 (HT 60)	20	0·17	0·53	1·24	0·013	0·011	0·22	0·11	0·14						38·6	63·5	31·0
C	HW 40 (HT 60)	25	0·14	0·29	1·23	0·011	0·003	0·10				0·08				49·7	59·1	19·0
D	HW 63 (HT 70)	20	0·16	0·36	0·92	0·012	0·013	0·80	0·38	0·21	0·35					69·8	79·4	35·3
E	HW 50 (HT 70)	25	0·15	0·30	1·13	0·012	0·005	0·24	0·82	0·40	0·26	0·026	0·0028	0·014		64·5	73·9	19·0
F	HW 70 (HT 80)	19	0·15	0·26	0·75	0·013	0·009	0·28	1·38	0·61	0·48	0·07	0·0014			76·3	81·7	22·5
G	HW 80 (HT 80)	20	0·15	0·24	1·28	0·022	0·013	0·23	0·23	0·50	0·49			0·003	0·002	73·8	83·4	16·0
H	HW 90 (HT 100)	25	0·15	0·25	0·82	0·009	0·007	0·24	0·93	0·54	0·54	0·06				98·2	102·3	20·0
I	HW 90 (HT 100)	13	0·15	0·25	0·82	0·009	0·007	0·24	0·93	0·54	0·54	0·06				98·7	102·1	23·9
J	QT Al-kill. 33	25	0·10	0·26	1·18	0·010	0·003									38·6	49·1	29·8
K	QT Al-kill. 37	20	0·11	0·25	1·25	0·010	0·008		0·57							37·0	51·6	45·0
L	QT Al-kill. 58	25	0·10	0·18	0·54	0·010	0·009		2·50	0·35	0·41					61·2	68·4	31·2
M	2·5% Ni	20	0·09	0·27	0·55	0·009	0·008	0·50	2·55	0·035	0·006			0·010	0·0092	37·1	47·5	31·0
N	3·5% Ni	20	0·06	0·30	0·51	0·011	0·007		3·53					0·027		38·2	49·3	30·0
P	9% Ni	20	0·07	0·20	0·48	0·008	0·017	0·18	8·54					0·017	0·011	67·2	71·0	25·5
Q	Semi killed	25	0·19	0·07	0·71	0·022	0·015									27·0	45·0	26·0
R	HW 50 (HT 60)	25	0·15	0·40	1·28	0·025					0·26	0·06				53·0	65·0	18·0
S	HW 63 (HT 80)	45	0·11	0·28	0·30	0·014	0·006	0·08	2·91	1·30	0·39			0·009		76·6	82·4	45·0
T	HW 70 (HT 80)	20	0·11	0·30	0·99	0·015	0·011	0·24	1·04	0·44	0·36					82·4	86·2	34·3

Table 2.
Chemical compositions and mechanical properties

Steel[a]	Kind of steel	Plate thick mm	Chemical compositions,[b] %													Mechanical properties		
			C	Si	Mn	P	S	Cu	Ni	Cr	Mo	V	B	Al	Nb	Y.P. (kg/mm²)	T.S. (kg/mm²)	Elong. (%)
A	HW 50 (HT 60)	25	0·13	0·43	1·22	0·019	0·014			0·21		0·06				52·0	64·0	42·0
B	HW 50 (HT 60)	25	0·15	0·26	1·22	0·012	0·013					0·064				53·0	64·0	23·2
C	HW 45 (HT 60)	28	0·14	0·36	1·21	0·011	0·010	0·07	0·50	0·04	0·097	0·034		0·029		58·8	68·9	27·0
D	HW 50 (HT 60)	28	0·16	0·39	0·77	0·010	0·012	0·34				0·030		0·034		60·6	68·5	28·5
E	HW 50 (HT 60)	30	0·12	0·36	1·21	0·017	0·011	0·21	0·21	0·12	0·03			0·039		53·0	63·7	47·6
F	HW 50 (HT 60)	25	0·13	0·33	1·51	0·024	0·014	0·04	0·21	0·03	0·13					55·0	68·5	
G	HW 45 (HT 60)	25	0·15	0·47	1·37	0·015	0·008	0·07	0·02		0·05	0·046		0·01	0·038	47·7	64·6	24·5
H	HW 63 (HT 70)	40	0·13	0·41	1·02	0·013	0·012	0·21	1·19	0·39	0·30	0·01		0·010		65·7	76·8	25·0
I	HW 70 (HT 80)	25	0·14	0·31	1·47	0·010	0·005	0·10			0·61		0·003	0·056	0·040	78·2	82·3	18·3
J	HW 70 (HT 80)	28	0·12	0·27	0·86	0·006	0·004	0·26	0·80	0·47	0·45	0·043	0·0025	0·032		85·0	89·0	25·0
K	HW 70 (HT 80)	20	0·12	0·22	0·95	0·026	0·017	0·29	0·90	0·65	0·54	0·06	0·003			84·2	87·8	28·0
L	HW 70 (HT 80)	20	0·11	0·30	0·99	0·015	0·11	0·24	1·04	0·44	0·36					82·4	86·2	34·3
M	HW 90 (HT 100)	20	0·15	0·24	0·78	0·013	0·009	0·17	1·26	0·70	0·55	0·07				101·9	105·7	22·0
N	QT Al-kill. 33	19	0·09	0·29	1·17	0·011	0·005									36·0	49·0	48·0
P	9% Ni[c]	13	0·07	0·26	0·48	0·016	0·010	9·38								69·0	74·4	26·8

a. Steels except *G* are quenched and tempered.
b. Check analysis.
c. Ladle analysis instead of check analysis.

Table 3.
Maximum tensile residual stress for various high strength steels

	σ_y[a]	σ_1[b]	σ_1/σ_y	σ_2[c]	σ_2/σ_y
HT 60	50	42	0·84	53·7	1·08
HT 70	60	44	0·73		
HT 80	70	45	0·64	47·5	0·69
HT 100	90	48	0·53		

a. Guaranteed yield point.
a, b, c in kg/mm².

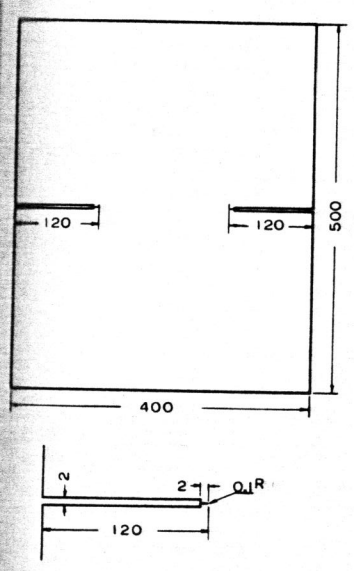

Fig. 1. Deep notch test specimen.

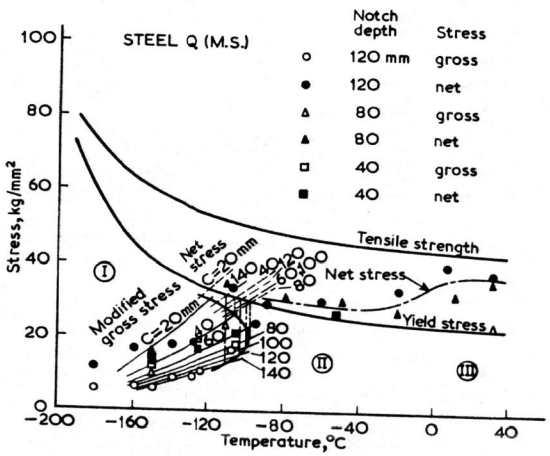

Fig. 2. Fracture initiation characteristics for mild steel, Steel Q.

Fig. 3. Fracture initiation characteristics for 60 kg/mm² high strength steel, Steel R.

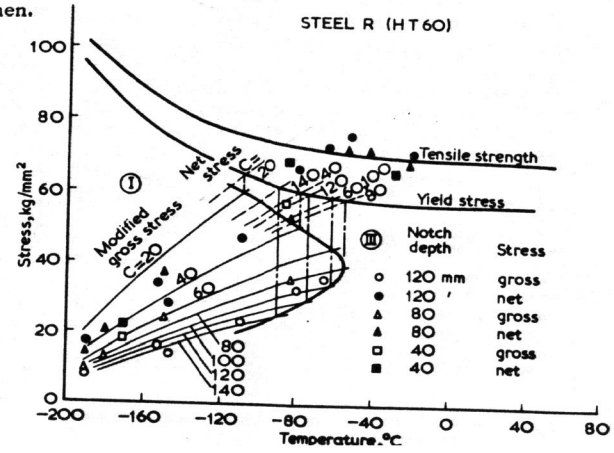

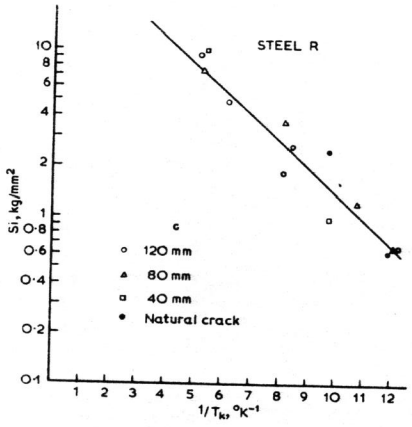

Fig. 4. Correlation between plastic surface energy for brittle fracture initiation and absolute temperature, Steel R.

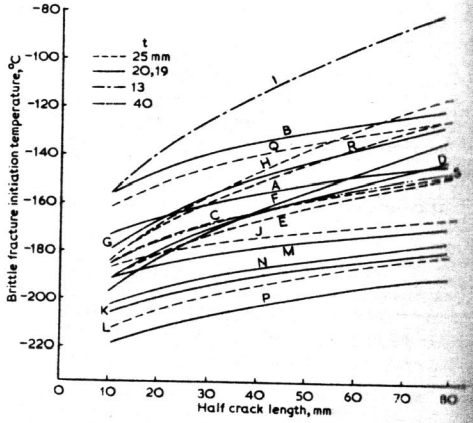

Fig. 5. Correlation between brittle fracture initiation temperature and half crack length in infinite plate for various steels.

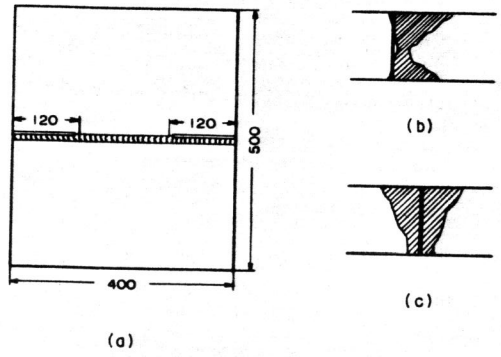

Fig. 6. Welded deep notch test specimen, and locations of notch along bond and in weld metal, respectively.

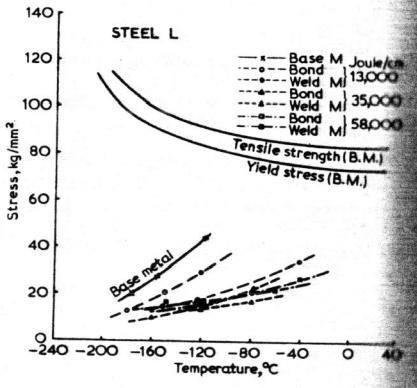

Fig. 7. Brittle fracture initiation characteristics of base metal and welded joint deposited by manual and automatic weldings (c = 120mm, 80 kg/mm² high strength steel, Steel L).

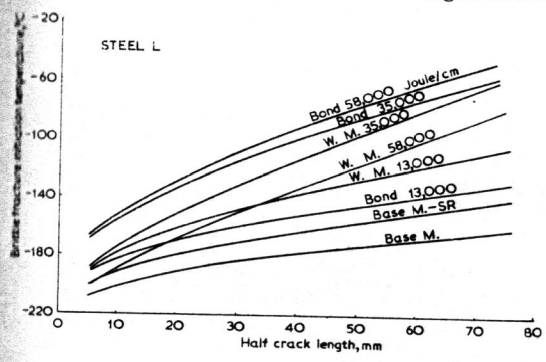

Fig. 8. Correlation between brittle fracture initiation temperature and half crack length of base metal and welded joint deposited by manual and automatic welding for 80 kg/mm² high strength steel. Steel L in Table 2 (where, $\sigma = \sigma_y/2{\cdot}5$).

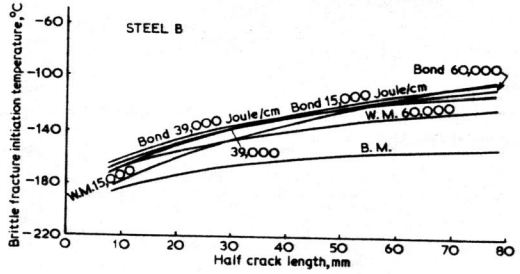

Fig. 9. Correlation between brittle fracture initiation temperature and half crack length for HT60 (Steel B in Table 2, $\sigma = \sigma$ /2·5).

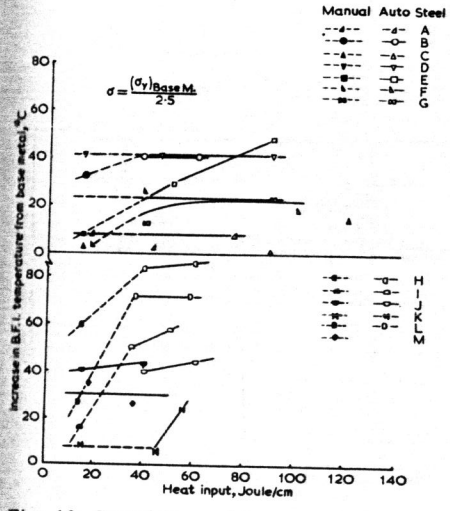

Fig. 10. Correlation of increase in brittle fracture initiation temperature of bond from base metal, $[\Delta T_t]_{c-40}$, and heat input ($\sigma = \sigma_y$ base metal/2·5).

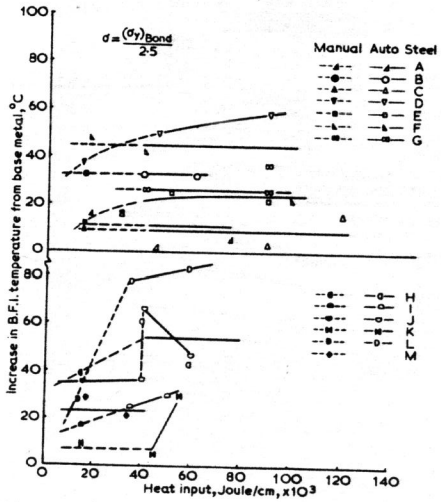

Fig. 11. Correlation of increase in brittle fracture initiation temperature of bond from base metal, $[\Delta T_t]_{c-40}$, and heat input ($\sigma = \sigma_y$ bond/2·5).

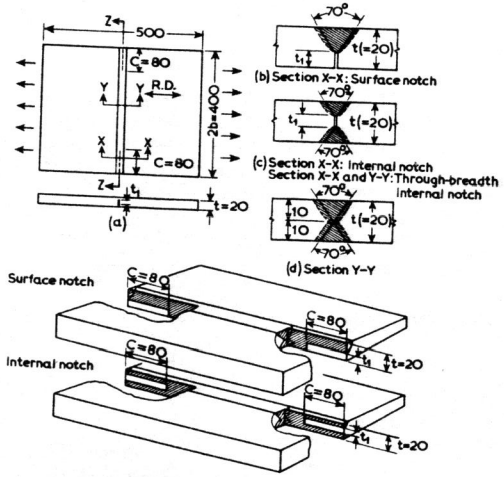

Fig. 12. Deep notch test specimens with surface and internal notches.

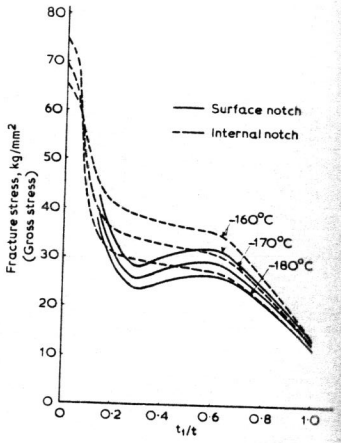

Fig. 14. Correlation between fracture stress (gross) and t_i/t for surface and internal notches.

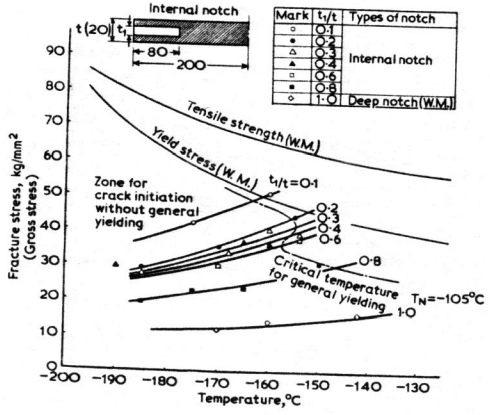

Fig. 13. Correlation between fracture stress (gross) and temperature for various internal notches.

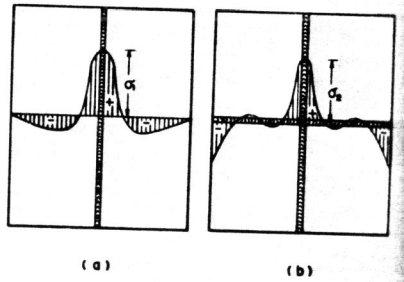

Fig. 15. Welding residual stress distribution (a) longitudinal joint (b) cross joint.

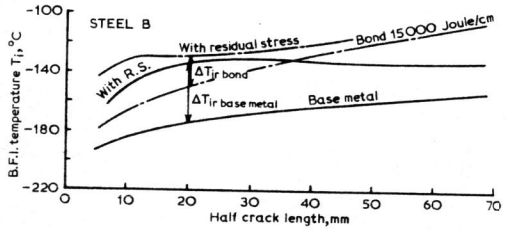

Fig. 16. Effect of welding residual stress on correlation between brittle fracture initiation and half crack length (Steel B in Table 2, $\sigma = \sigma_y/2{\cdot}5$).

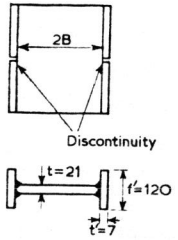

Fig. 17. Longitudinally welded I-type test specimen.

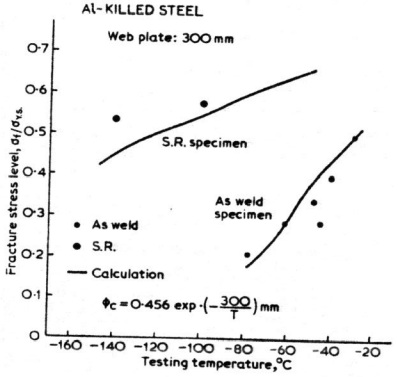

Fig. 18. Results of longitudinally welded I-type tests relation between fracture stress level and testing temperature.

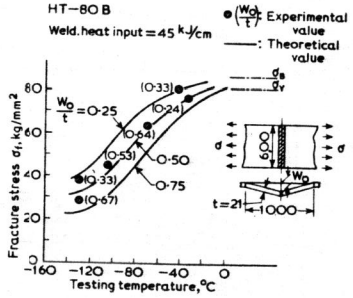

Fig. 19. Correlation between fracture stress and temperature in welded wide plate specimen with angular distortion.

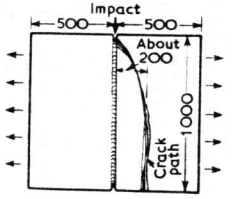

Fig. 20. Crack path in welded specimen for mild steel [12].

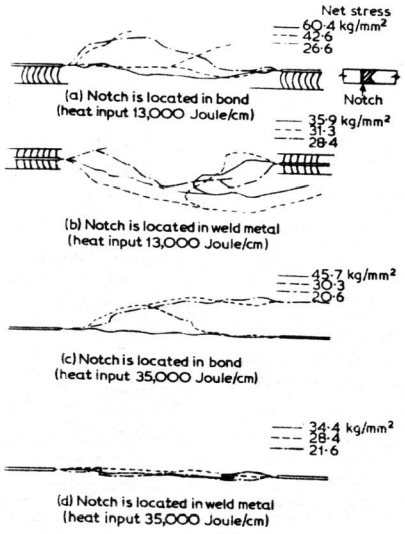

Fig. 21. Crack path in welded specimen for HT80 (Steel L in Table 2).

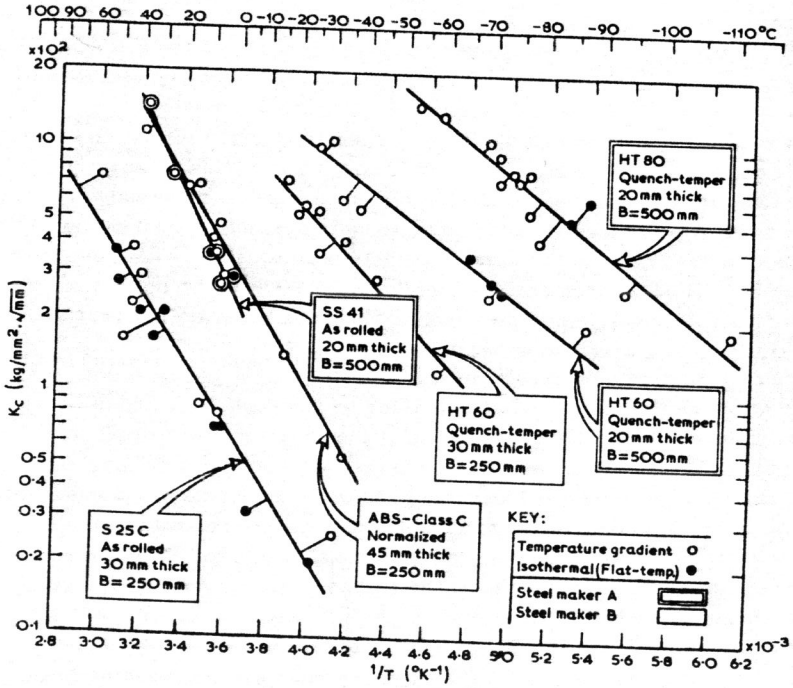

Fig. 23. $k_c \sim 1/T_K$ relationship in double tension test for various kinds of steel.

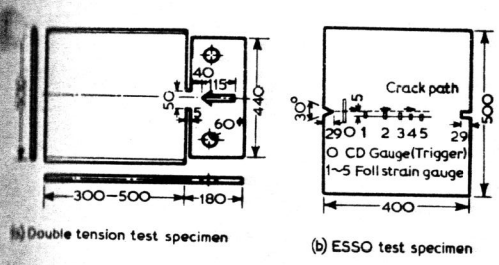

Fig. 22. Specimen for brittle fracture arresting characteristics.

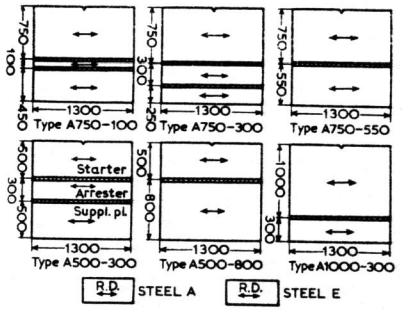

Fig. 25. Crack arrester test specimen.

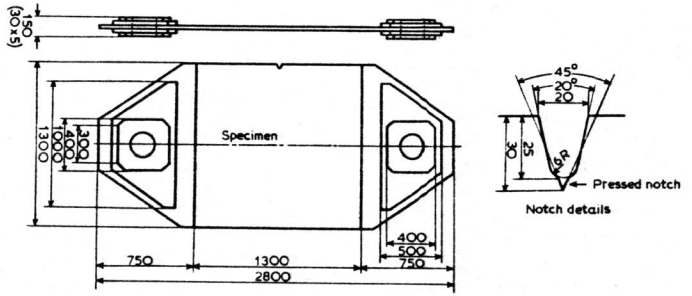

Fig. 24. Crack arrester test specimen, pull plate and details of notch.

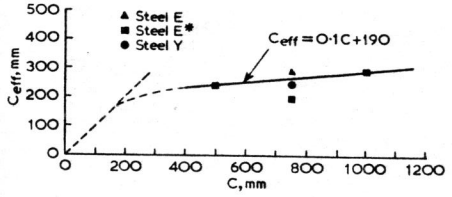

Fig. 26. Correlation between effective crack length and actual crack length.

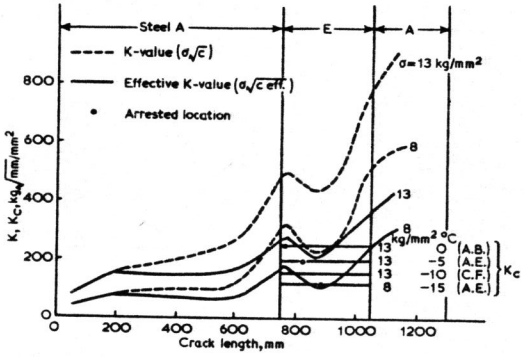

Fig. 27. Correlation between K, K_c and crack length (A750-300).